J Solid State Electrochem (2004) 8: 842–853
DOI 10.1007/s10008-004-0552-7

ORIGINAL PAPER

Ulrich Hasse · Klaus Wagner · Fritz Scholz

Nucleation at three-phase junction lines: in situ atomic force microscopy of the electrochemical reduction of sub-micrometer size silver and mercury(I) halide crystals immobilized on solid electrodes

Received: 15 January 2004 / Accepted: 23 March 2004 / Published online: 7 August 2004

Abstract The electrochemical reduction of sub-micrometer size silver halide crystals immobilized on the surface of gold and platinum electrodes starts at the three-phase junction line where the three phases "metal", "silver halide" and "electrolyte solution" meet. Following nucleation at this line the reaction advances within seconds on the surface of the silver halide crystals until the entire surface is covered with about 20 atomic layers of silver and the reduction is terminated. The silver layer can be oxidized anodically and the next layer of the silver halide crystals becomes accessible for further reduction. This sequence of reductions and oxidations can be repeated. The nucleation of silver at the three-phase junction line can be detected by atomic force microscopy (AFM) measurements when, after a short reduction pulse and dissolution of the remaining silver halide, a thin ring of silver is observed at the place where the three-phase junction line was situated. The entire scenario of electrochemical reduction of immobilized silver halide crystals depends on the crystal size. Large crystals (about 100 μm edge-length) immobilized on the surface of optically transparent indium tin oxide electrodes show the growing of silver whiskers on the crystal surface, similar to what is known for the reduction of silver halides with photographic developers. However, also in the case of the large crystals, the reduction starts at the three-phase junction line. The electrochemical reduction of immobilized sub-micrometer size crystals of Hg_2Cl_2 and Hg_2Br_2 starts also at the three-phase junction. In the case of gold electrodes the formation of liquid mercury is followed by the formation of a solid crystalline gold amalgam. In the case of platinum electrodes the liquid mercury wets the platinum surface but does not destroy it.

Keywords Atomic force microscopy · Indium tin oxide electrodes · Electrochemistry · Silver halides · Mercury(I) halides

U. Hasse · F. Scholz (✉)
Universität Greifswald,
Institut für Chemie und Biochemie,
Soldmannstrasse 23,
17489 Greifswald, Germany
E-mail: fscholz@uni-greifswald.de
Tel.: +49-3834-864450
Fax: +49-3834-864451

K. Wagner
Agfa Gevaert AG, Werk Leverkusen,
Kaiser-Wilhelm-Allee,
51301 Leverkusen, Germany

Introduction

The electrochemical conversion of one crystalline compound into another is a fascinating area of research, since it addresses such questions as how and where the reaction starts and how it proceeds through the crystal. Atomic force microscopy (AFM) [1] is well suited to study such reactions under in situ conditions. A number of AFM studies have been published so far, e.g., on fullerenes [2], solid 7,7,8,8-tetracyanoquinodimethane [3], lead oxides [4], and goethite crystals [5]. We decided to study the reduction of silver and mercury(I) halide crystals because these metal–metal halide systems are chemically and electrochemically reversible. Furthermore, silver halides play the key role in photography. Although their importance is certainly decreasing, they have been extensively studied in the past with respect to properties and reactions. In the photographic literature [6, 7, 8, 9], two terms are used to designate different pathways of the reduction process: the term "physical development" describes the process when the silver halide crystal is slightly soluble in the developer solution and the silver crystals grow, ideally surrounded only by solution, starting at a nucleus in the solution. The term "chemical development" describes a reduction pathway where the metallic silver grows, usually in the form of wires (whiskers), directly at the silver halide surface,

presumably due to a diffusion of silver ions via Frenkel defects in the crystal. The development of the latent image by application of a reducing agent to the silver halide emulsion always leads to filamentous silver grains. The formation of silver grains starts at the nuclei of silver atoms at the surface of the silver halide crystals. In the case of sub-micrometer size silver halide crystals immobilized on gold electrodes and in contact with an electrolyte solution, the conditions are rather different. Here we can show that the entire three-phase junction line where the three phases "metal", "silver halide" and "electrolyte solution" meet acts as a locus of nucleation. The reduction of the silver halides produces a silver layer that grows, starting at the three-phase junction line, around the crystals until they are covered by a tight layer of metallic silver. When silver halide crystals that are larger than a micrometer are immobilized on optically transparent indium tin oxide (ITO) electrodes, the reduction proceeds as under photographic conditions, i.e., filamentous silver grows on the crystal surface, although the reduction also starts at the three-phase junction.

In the case of the immobilized sub-micrometer size crystals of mercury(I) halides, the reduction also starts at the three-phase junction line and produces liquid mercury that reacts in the case of a gold electrode with the underlying gold to form a solid crystalline amalgam, whereas in the case of a platinum electrode, it only wets the surface.

Materials and methods

Instrumentation and electrodes

All measurements were performed with an atomic force microscope/scanning tunnelling microscope (AFM/STM) of Digital Instruments (hardware: NanoScope Version 1.0, software: NanoScope E Version 4.23r3). A Styropor box acoustically shielded the microscope and a self-designed table served for damping of vibrations [4]. The electrochemical cell was externally controlled by a μ-AUTOLAB (EcoChemie, Netherlands).

For the in situ AFM-electrochemistry of immobilized sub-micrometer particles, very smooth electrodes are necessary; however, atomically flat electrodes did not serve the purpose because it was impossible to immobilize the crystals on surfaces so smooth. It turned out that electrodes consisting of a gold layer covering a chromium layer on quartz plates were highly useful. These electrodes were purchased from Schröer (Lienen, Germany). The surface roughness of these electrodes is just sufficient to support the immobilization of well-separated crystals. A self-made reference electrode based on Ag/AgCl (3 M aqueous KCl) was used and all potentials given in this paper refer to this electrode. The electrode was small enough to be directly connected with the electrochemical cell for in situ AFM [5].

A special electrochemical cell was used to observe (with the help of an optical microscope) the course of electrochemical reduction of silver halide crystals with an edge length above 100 μm. The silver halide crystals were immobilized on the surface of an optically transparent ITO electrode (polished float glass, SiO_2 passivated, resistance 4–8 Ω, Delta Technologies, USA). The ITO electrode formed the bottom of the electrochemical cell and the microscope was in a reversed position to enable an observation of the crystals from underneath. A Leitz Laborlux 12 POL S light microscope (Leica, Germany) with a 100 W halogen incandescent lamp was used. The magnification was 100-fold.

Chemicals

The silver bromide (with 5 mol% iodide) samples were kindly provided by Agfa (Leverkusen, Germany) as raw emulsion without chemical surface treatment. Potassium chloride, bromide and iodide, mercury(I) nitrate and silver nitrate (all p.a.) were from Merck (Darmstadt, Germany).

Preparation of silver halide crystals

Silver halide crystals with well-developed crystal shape and a size that allows AFM imaging To prepare silver halide crystals with well-developed crystal shape and a size that allows AFM imaging, i.e. with an edge length between 400 and 800 nm, different strategies were followed. All experiments were performed in a darkroom to avoid the formation of silver seeds at the surface.

-1. Both 10 ml of a solution of silver nitrate and of potassium halide in water (both 0.1 M) were simultaneously added at a rate of one drop per second to a solution of 5 g gelatine in 200 ml water at room temperature (double jet technique). To control the mixing rate a syringe system (sampling unit 708, Metrohm, Switzerland) was used. During the addition, the solution was vigorously stirred with a magnetic bar. After completion of the addition of both solutions, the suspension was stirred for 30 min at room temperature before the silver halide precipitate was filtered off. To remove the adjacent gelatine, the silver halide precipitate was suspended in water and filtered off, 50 times in all. Eventually, the crystals were dried at 40 °C.
-2. An aqueous 0.1 M solution of silver nitrate (100 ml) was slowly added to 100 ml of an aqueous 0.1 M solution of oxalic acid at 80 °C. This leads to a reductive precipitation of silver particles with an average diameter of 100–500 nm. The silver particles were suspended either in acetonitrile or water depending on the following applications. Two different ways to convert the silver particles to silver halide crystals were followed:

-a. Evaporation of a suspension of silver particles on the gold electrode to immobilize the silver particles on the surface. Following the evaporation of the acetonitrile, a saturated aqueous solution of the halogen was put on the surface of the electrode. The halogens oxidize the silver particles and form silver halide crystals that stick to the surface of the gold electrode. After a reaction time of 5 min, which is sufficiently short as not to destroy the gold electrode, the solution was removed and the electrode was washed and dried at 80 °C for 30 min. This procedure resulted in very flat crystals sticking to the gold electrode.
-b. Addition of a saturated aqueous solution of the halogen to a suspension of silver particles in water. After a reaction time of 12 h the product was filtered off, suspended in water and immobilized on the gold electrode by evaporation of an appropriate suspension as previously described. This leads to well-developed crystals that do not exhibit the flat shape of the crystals prepared according to 2a.

All preparation steps were performed under a nitrogen blanket to avoid the formation of an oxide layer on the silver particles, because this could impede the oxidation of the silver by the halogens.

Silver halide crystals suitable for light microscopy To prepare silver halide crystals that are suitable for light microscopy, i.e. crystals with an edge length of more than 100 μm, the following procedure was followed: silver halide crystals with an average edge length of 200–300 nm were suspended in water and the suspension was kept at 80 °C for 40 h. Instead of water, acetonitrile can be used with the same results provided that the temperature is kept at 60 °C.

Cleaning the crystals Commercial silver bromide/iodide suspensions that are used in film materials contain up to 5% gelatine and some additives to prevent biological fouling. To clean the crystals with respect to these additives and gelatine, 1 g of the commercial suspension was added to 50 ml boiling water and the crystals were separated by centrifugation at 2,500 rpm for 120 s. This process was repeated 50 times.

Preparation of the mercury(I) halide crystals

To 50 ml of a 0.1 M mercury(I) nitrate solution 50 ml of a 0.1 M potassium chloride (bromide) solution were dropwise added under stirring at room temperature. The suspension formed was stirred for another 5 min and then the precipitate was filtered off. The precipitate was washed 10–15 times with distilled water and dried at 60 °C.

Immobilization of the silver and mercury(I) halide crystals

To immobilize crystals with a size below 5 μm, a suspension of silver halide in acetonitrile was used. The suspension was prepared as follows: About 0.5 g of the halide was suspended in 10 ml acetonitrile. After waiting 5 min to allow most of the suspended crystals to sediment, 30 μl of the supernatant were sampled with a syringe and diluted with 120 μl of acetonitrile. The resulting suspension was placed on the gold electrode and the acetonitrile was allowed to evaporate slowly at room temperature within 5–10 min.

Results and discussion

Silver halides

In situ AFM of electrochemical reduction of pure self-prepared silver halide crystals (AgCl, AgBr, AgI) AgCl and AgBr crystals of sub-micrometer size immobilized on a gold electrode were reduced at a potential of −600 mV and AgI at −700 mV. As electrolyte, a 0.1 M solution of the corresponding potassium halide was used. A short reduction pulse of 5 s was applied before the AFM image was recorded under open potential conditions. This sequence was repeated until the AFM image did not change anymore, i.e., until the volume of the crystal did not change anymore. The volume of the crystals was evaluated from the AFM images by integration. Figure 1 shows a crystal of silver bromide (a) before the reduction and (b) after the reduction at −600 mV. The volume of the crystal shrank by 32% only (the volume was determined with the help of the software NanoScope E Version 4.23r3). If the entire crystal had been reduced the volume decrease would have to be 76%. Obviously, the reduction process stopped before the entire crystal was completely reduced, and it was assumed that the crystal was covered by a compact metallic silver layer. Therefore, a potential of +300 mV was applied to anodically dissolve the silver layer. After this oxidative dissolution of the silver layer a sequence of reductive pulses was again applied and the AFM images were recorded until again a constant crystal image and volume were observed. This cycle of oxidation and reduction could be repeated up to five times. The experiments indeed showed that the silver halide crystals can only ever be reduced on the surface, since a tight metallic silver layer is formed that finally terminates the reduction. In other words, a silvering of the surface of the crystals was achieved. Interestingly, the thickness of the silver halide layers reduced to silver is rather constant for each silver halide, in the case of AgCl about 8.0 nm, for AgBr about 8.8 nm, for AgI about 9.5 nm, and for $AgBr_{0.95}I_{0.05}$ about 9.14 nm (cf. Table 1). This means that, on average, the silver layer consists of about 20 atomic layers (see Table 2). The

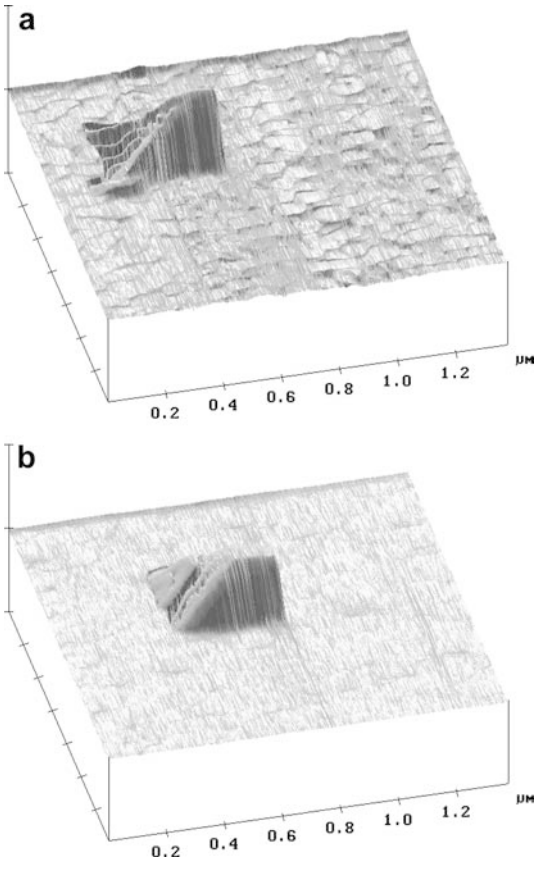

Fig. 1a, b Atomic force micrographs of a silver bromide crystal immobilized on a gold electrode in 0.1 M potassium bromide solution. **a** Before the reduction. **b** After a reduction at −600 mV

experimental results of a layer-by-layer reduction of the immobilized silver halide crystals can be explained by two models: in the first model it may be assumed that the reduction starts at the entire silver halide | solution interface (see Fig. 2a) and advances into the crystal until complete coverage of the surface by a compact metallic silver layer. This route can be followed only when the silver halide would have a sufficient electronic conductivity. In the second model (see Fig. 2b) it is assumed that the reduction starts at the three-phase boundary line silver halide–gold–electrolyte solution, and advances along the surface of the crystal until the entire crystal is covered with a compact metallic silver layer. From the AFM images taken in the course of reductions it was impossible to discern what route the reaction really follows. Therefore, the following experiment was performed: AgBr crystals were reduced at −600 mV for 1 s, which is insufficient to reach a compact silver layer, as was known from the previously described experiments. This reduction was performed in a special flow-through cell that allowed exchange of the solution without "loosing" the crystal in the AFM. After the reduction, the solution was exchanged with a 5 M ammonia solution. After waiting for 5 min to give the remaining silver halide a chance to dissolve, an AFM image was recorded. Figure 3a shows the silver halide crystal before the reduction pulse was applied and Fig. 3b shows the silver that was left on the electrode after the silver halide was dissolved by ammonia. Clearly, a ring structure is observed that can only be silver that was formed during the short reduction pulse. If the model shown in Fig. 2a was operative it would be incomprehensible that the silver atoms would arrange in this ring structure, whereas with the model depicted in Fig. 2b this finding is easily understood, because the silver ring is exactly at the place of the three-phase boundary line. Having obtained these results on the electrochemical reduction of silver bromide immobilized on the surface of a gold electrode, it was interesting to compare this scenario with what happens when the reduction is caused by a chemical reagent, i.e., a usual chemical developer. Figure 4a shows a silver bromide crystal immobilized on the gold electrode and covered by water and Fig. 4b shows the same crystal after chemical reduction with the commercial developer Photo-Rex after an exposure to the reductant for 60 s. Quantification of the volume decrease gave the result that the crystal shrank by 75%. This is almost the theoretical value of 76% for a complete reduction of a silver bromide crystal to a silver metal crystal. Two facets of these results are important: (1) the entire silver bromide crystal was reduced within a rather short time period, and (2) no disintegration of the silver bromide crystal took place, but a compact silver crystal was formed as if the silver bromide did simply shrink down to the metal. The action of the underlying gold electrode can be understood in terms of the Gurney-Mott theory of development: "The condition that any speck may act as a nucleus for development, then, is that its vacant electronic levels shall be low enough to charge up negatively from the developer in use. This theory suggests that any singularity on the surface of a grain will act as a latent image if it provides a sufficiently deep potential hole" [10]. Of course, the gold electrode is nothing but a very large "speck" on the surface of the grain.

In the course of these experiments, some other interesting observations were made: when gold electrodes with immobilized silver bromide crystals were kept for some days in the normal laboratory air, the formation of silver whiskers was observed. Figure 5 gives an example. This whisker formation was not observed when the gold electrodes were kept under

Table 1 The thickness of the layers of silver halide crystals that can be reduced until the reduction is terminated by the formation of a compact metallic silver layer. The reduction was performed at −600 mV (−700 mV in case of $AgBr_{0.95}I_{0.05}$). The silver layers were anodically oxidized at +300 mV before the next layer of the silver halide could be reduced

Silver halide	Thickness of the reduction layer(nm)
AgCl	7.75; 8.12; 8.22; 8.15; 7.99
AgBr	8.65; 8.7; 8.85; 8.93; 8.92
AgI	9.88; 9.08; 9.45; 9.76; 9.55
$AgBr_{0.95}I_{0.05}$	9.04; 8.99; 9.12; 9.55; 9.02

Table 2 Database for calculation of the average thickness of the silver layer formed upon reduction of silver halides

	AgCl	AgBr	AgI	$AgBr_{0.95}I_{0.05}$
M (g/mol)	143.323	187.774	234.774	190.130
ρ (g/cm^3)	5.560	6.473	6.010	6.4811*
ρ/M (mol/nm^3)	3.879349×10^{-23}	3.447229×10^{-23}	2.559909×10^{-23}	3.408773×10^{-23}
ρ^a/M (atoms/nm^3)	23.4	20.8	15.4	20.5
Average thickness of reduced layers (nm)	8.0	8.8	9.5	9.14
Number of silver atoms per nm^2	187.2	183.0	146.3	187.4
Number of layers of silver atoms assuming 9 atoms per nm^2	20.8	20.3	16.2	20.8

[a]This density was calculated from the lattice constants $a(\text{Å}) = 5.7748 + 3.68\cdot10^{-3}c_{AgI}$, with c_{AgI} being the concentration of AgI in the solid solution in mol%, according to [21]

nitrogen or in a desiccator above P_2O_5. When silver bromide crystals were dissolved with an ammonia solution after such partial reduction in the laboratory environment, again ring structures became visible, and very surprisingly, the gold layer around the silver bromide crystals was obviously dissolved (Fig. 6). These results can be explained as follows: the silver bromide crystals are reduced by reductants that are present in ordinary laboratory air, e.g., ethanol vapours. This reduction starts at the three-phase boundary line probably because oxidation of the reductant occurs at the gold surface and the reduction of the silver ions occurs at the nearest place, i.e. the edge of the crystal adjacent to the gold. The formation of whiskers on the surface of the silver halide crystal may have the same origin or it may start at the interface silver halide | air. The reduction of the silver bromide must release bromide anions and also protons to the water film that always covers the surface. The protons result from oxidation of the reductant. In acidic bromide solution, oxygen is strong enough to oxidize bromide to bromine [11], and this bromine can oxidize gold. Hence, the dissolution of the gold will be the result of the bromine formation around the silver halide crystals. This scenario can explain the experimental findings. To test the explanation, gold electrodes with immobilized silver bromide crystals were kept for 7 days in air that was saturated with ethanol vapour, in a nitrogen atmosphere saturated with ethanol vapour, and in air without organic vapours. Only the electrode kept in ethanol vapour *and* air exhibited the described features!

In situ AFM of electrochemical reduction of commercial silver bromide crystals with 5 mol% iodide Silver bromide crystals of the composition $AgBr_{0.95}I_{0.05}$ were separated from the commercial gelatine suspension and immobilized on the gold electrode as described in Materials and methods. Figure 7a depicts the AFM image as recorded before the electrochemical reduction. The latter was performed at −700 mV for 10 s. This reduction period was followed by recording of an AFM image. Then another reduction was performed for 10 s, and the next AFM image was recorded (Fig. 7b). This was repeated until the shape and volume of the crystal did not change anymore. In these experiments it turned out that the commercial $AgBr_{0.95}I_{0.05}$ crystals behave exactly in the same way as the self-prepared pure silver halide crystals, i.e., the reduction leads to the formation of a compact silver layer that finally interrupts the reduction because it completely covers the silver bromide crystal. When the silver layer was anodically dissolved in a 0.1 bromide solution and the remaining

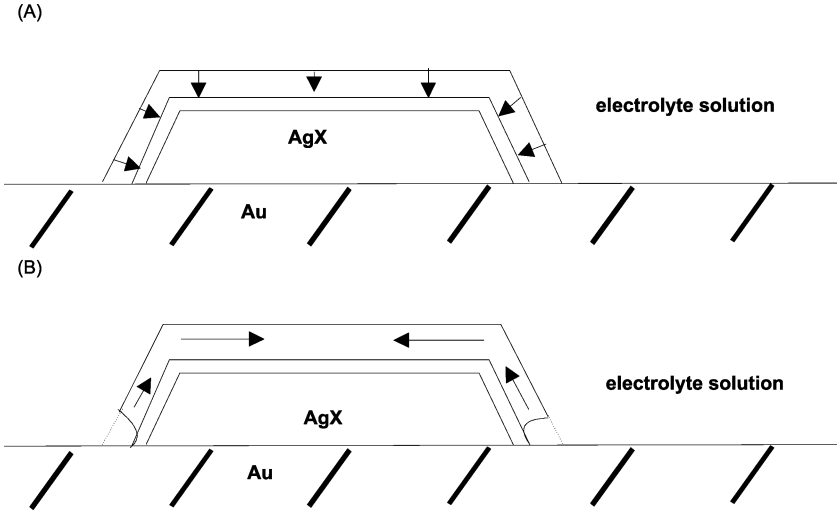

Fig. 2a, b Schematic model for the reduction of a silver halide crystal immobilized on a gold electrode and adjacent to an electrolyte solution. **a** The reduction starts at the entire silver halide | electrolyte solution interface. **b** The reduction starts at the silver halide-gold-electrolyte solution three-phase boundary line and advances along the surface

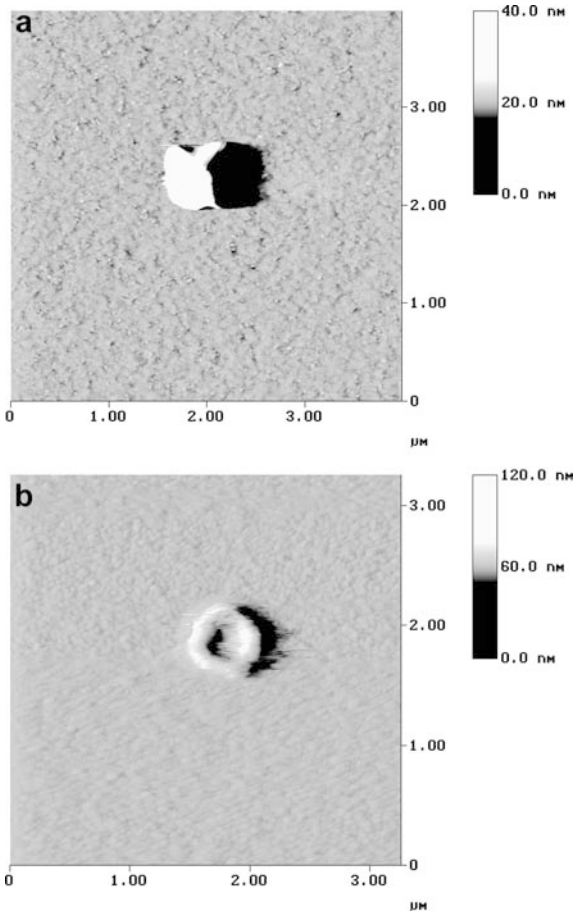

Fig. 3a, b Atomic force micrographs of a silver bromide crystal immobilized on a gold electrode in 0.1 M potassium bromide solution. **a** Before the reduction. **b** After a reduction at −600 mV for 1 s and the dissolution of the remaining silver bromide with 5 M ammonia

$AgBr_{0.95}I_{0.05}$ crystal was again reduced as far as possible, a layer-by-layer reduction and oxidation could be achieved as described for the self-prepared crystals. Table 1a gives the thickness of the layers of the $AgBr_{0.95}I_{0.05}$ crystals that could be reduced until the reduction stopped. The average thickness of 9.14 nm of the $AgBr_{0.95}I_{0.05}$ crystal indicate the formation of about 20 atomic layers of silver, i.e. this is the same number as in the case of AgCl and AgBr and only slightly more than for AgI. To investigate the starting point of the reduction, the $AgBr_{0.95}I_{0.05}$ crystal was reduced at −700 mV for 5 s and the remaining silver halide was dissolved in 5 M ammonia solution. Again, a ring structure was detected bearing witness to a reaction start at the three-phase boundary (cf. Figure 8). The main result of these experiments is that the commercial (photographic) $AgBr_{0.95}I_{0.05}$ crystals behave as do the self-prepared with respect to the pathway of electrochemical reduction. Figure 9 shows an AFM image of $AgBr_{0.95}I_{0.05}$ crystals after keeping them immobilized on the gold electrode for 1 week in laboratory air. Similarly to the experiments with pure silver bromide crystals, a dissolution of gold around the crystals was observed.

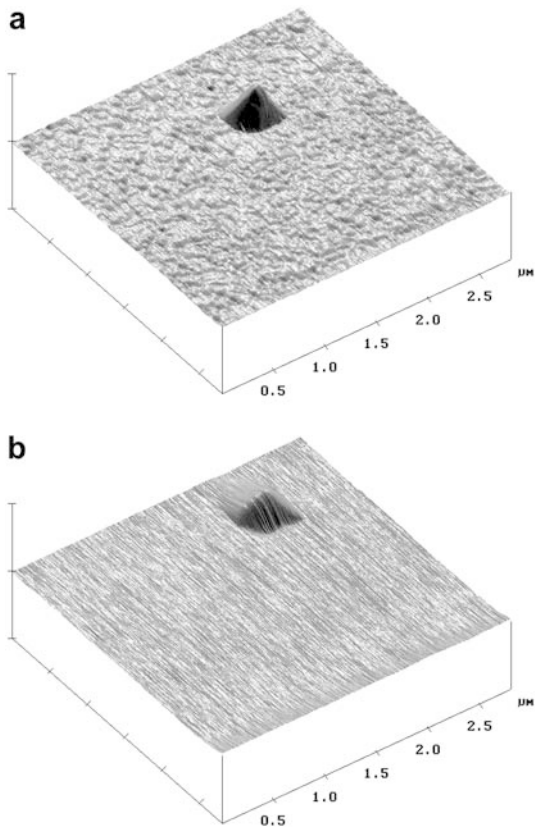

Fig. 4 **a** Atomic force micrograph of a silver bromide crystal immobilized on a gold electrode in water. **b** The same crystal after reduction with a photo developer for 60 s

Influence of light exposure on the reduction of silver halide crystals The described experiments have been repeated with silver halide crystals that were illuminated with a 200 W halogen lamp. The following electrochemical reduction process as monitored by AFM did not show any differences between illuminated and non-illuminated samples, although in chronoamperometry a much faster

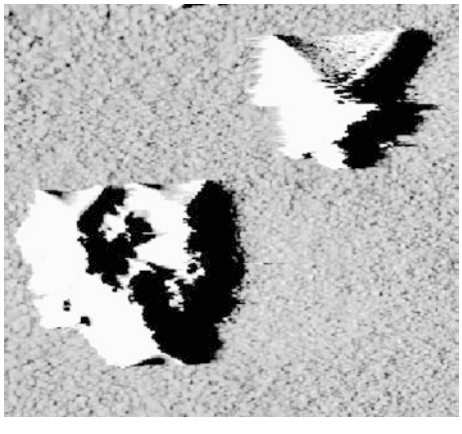

Fig. 5 Atomic force micrograph of a silver bromide crystal immobilized on a gold electrode after keeping for some days in laboratory air

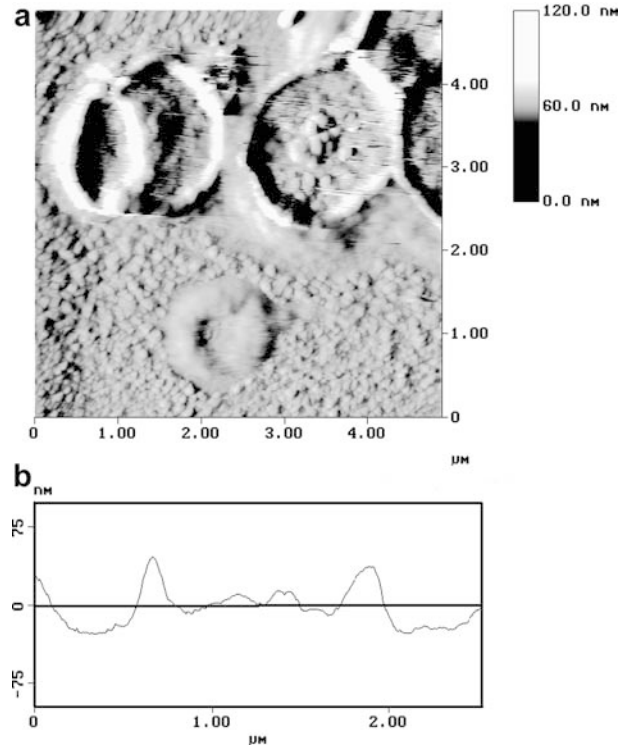

Fig. 6 **a** Atomic force micrograph of a gold electrode after keeping an immobilized silver bromide crystal for some days in laboratory air and dissolving the remaining silver bromide with 5 M ammonia. **b** Cut through the ring structure shown in **a**

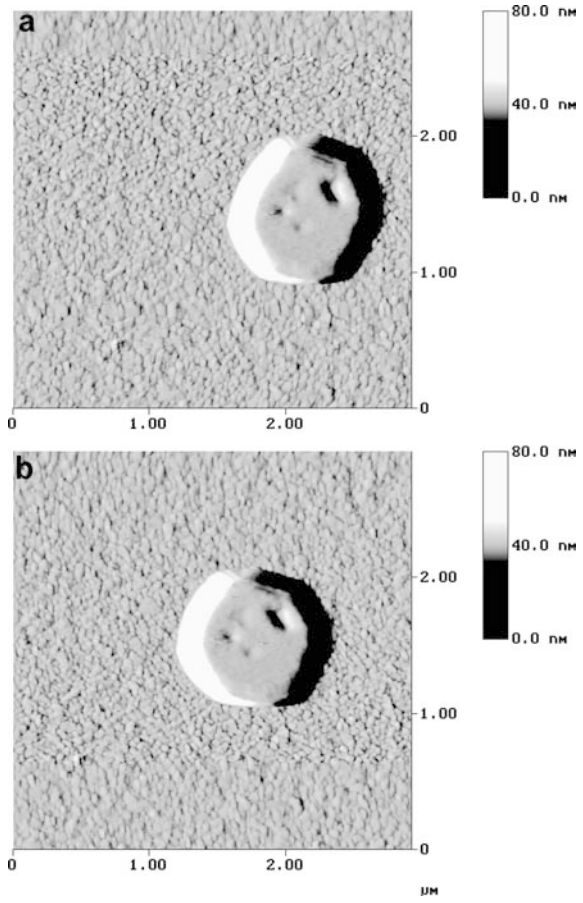

Fig. 7a, b Atomic force micrographs of a silver bromide crystal with 5 mol% iodide immobilized on a gold electrode in 0.1 M potassium bromide solution: **a** before and **b** after a reduction at −700 mV for 20 s

decay of reduction current was observed (not shown here). However, the geometric proceeding of the reduction was not altered. Since the illumination must have created nuclei, they are obviously not the active growing centres during the electrochemical reduction and the three-phase junction line is still the main locus of nucleation. Certainly, this may be a question of kinetics, in the way that silver layer growth starting at the three-phase junction line is much faster than the growth of the nuclei formed by illumination. The nuclei formed by illumination are certainly isolated from the gold surface and therefore not easily accessible by the electrons supplied via the gold electrode. The nuclei may still serve the job of increasing the rate of layer formation. The effect of illumination on the rate of reduction as measured in potential step chronoamperometric experiments will be the subject of further investigations.

Electrochemical reduction of large silver halide crystals followed by in situ optical microscopy Self-prepared silver bromide crystals with an edge length above 100 µm were immobilized on an optically transparent ITO electrode and the reduction was performed at a potential of −600 mV. The ITO plate was the bottom of the electrochemical cell and the microscope was reversed so as to allow following the course of reduction from underneath the cell. Figure 10 shows a typical picture of a partially reduced AgBr crystal. The growth of silver whiskers is clearly visible. This whisker growth could be seen in all cases of crystals of that size. In the case of very small crystals, i.e., those with an edge length around 1 µm, it was impossible to see the structure of the

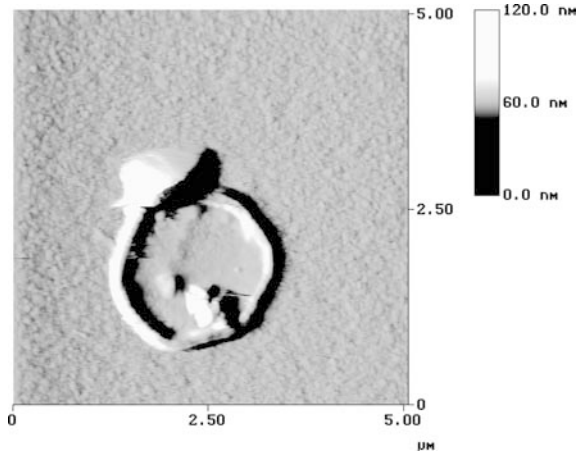

Fig. 8 Atomic force micrograph of a silver bromide crystal with 5 mol% iodide immobilized on a gold electrode after a reduction at −700 mV for 20 s and dissolving the remaining silver halide with 5 M ammonia

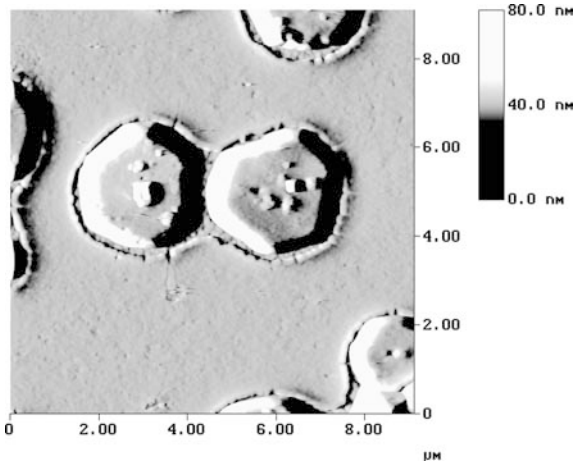

Fig. 9 Atomic force microscopy image of $AgBr_{0.95}I_{0.05}$ crystals immobilized on a gold electrode and kept for 1 week in laboratory air. The image was recorded with 0.1 M KBr solution as electrolyte

formed silver. These crystals simply blackened under the microscope.

Mercury(I) halides

Figure 11 shows Hg_2Cl_2 crystals immobilized on a gold electrode before and in the course of reduction at −700 mV. Between each image the crystal was reduced for 5 s. Already in Fig. 10b, c the formation of a flat mercury droplet that spreads on the gold surface is visible. The latter becomes very pronounced in Fig. 10d, e. There it is also visible that the gold layer around the droplets is disintegrating and obviously dissolving in the mercury droplets. Figure 11f, g, h finally shows that a crystalline compound is formed from the liquid mercury and the dissolved gold. Naturally, this can only be a gold amalgam. Figure 12 depicts a cut through a Hg_2Cl_2 crystal that was partially reduced to mercury. The arrows indicate the reaction front where the liquid mercury borders to the residual Hg_2Cl_2 crystal.

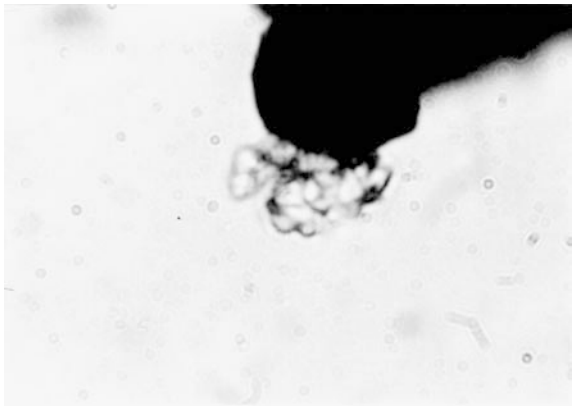

Fig. 10 Photography of a AgBr crystal immobilized on an optically transparent ITO electrode after a reduction at −600 mV for 200 s

Figure 13 shows Hg_2Cl_2 crystals immobilized on a platinum electrode before and in the course of reduction at −700 mV. Between each image the crystal was reduced for 5 s. The images show the formation of liquid mercury that is wetting single platinum crystal surfaces. This way the deposited mercury images the underlying platinum structure. Figure 13c shows the interesting effect that the crystal structure of the underlying platinum becomes more visible even at places where no immobilized Hg_2Cl_2 crystal were seen before the reduction. We suppose that at these places there have been extremely small crystals or even a film of Hg_2Cl_2 formed during evaporation of the suspension so that some small amounts of mercury could deposit at the supposedly free surface of the platinum. This deposition may also have enhanced the contrast of the AFM image. The experiments with Hg_2Br_2 crystals gave essentially the same results as those with calomel.

Conclusions

This study shows that the morphological pathway of reduction of silver halides depends to some extent on the size of the crystals. In the case of crystals that are smaller than 1 μm, only a surface layer of the crystals is reduced to a tight metallic silver layer, whereas much larger crystals exhibit the well-known growing of filamentous silver wires out of the crystal surface. This size-dependence was observed for silver halide crystals immobilized on gold and ITO electrodes under conditions of potentiostatic electrochemical reduction. The experimental results show that the electrochemical reduction starts at the three-phase junction line. It was impossible to discern any "point-like" nucleation sites at the three-phase junction line. Of course, such sites may exist but their activity could not be resolved on the time scale of the experiments. If they existed, the nucleation growth along the three-phase junction line must be much faster than the growth on the crystal-solution interface. Otherwise one would not see the rather regular ring structures as shown in Fig. 3b.

The major question that follows from the experimentally observed size dependence of the morphological pathway of reduction is, why whisker growth is observed in the case of large crystals and surface silvering in the case of very small crystals. Figure 14a depicts schematically how the surface silvering may be understood: at the front side of the silver layer the silver halide crystal is disintegrating, i.e., the halide ions are expelled to the solution and the silver ions diffuse to the metallic silver electrode. This process can be characterized by a specific flux of silver ions $f_{Ag^+,\,front}$. The reaction zone can probably be regarded, at least to some extent, as a mixed crystal (solid solution) of silver and the silver halide. In an earlier publication we have already had to make that assumption to model the reduction of silver halide crystals [12]. We believe that the whisker growth starts at

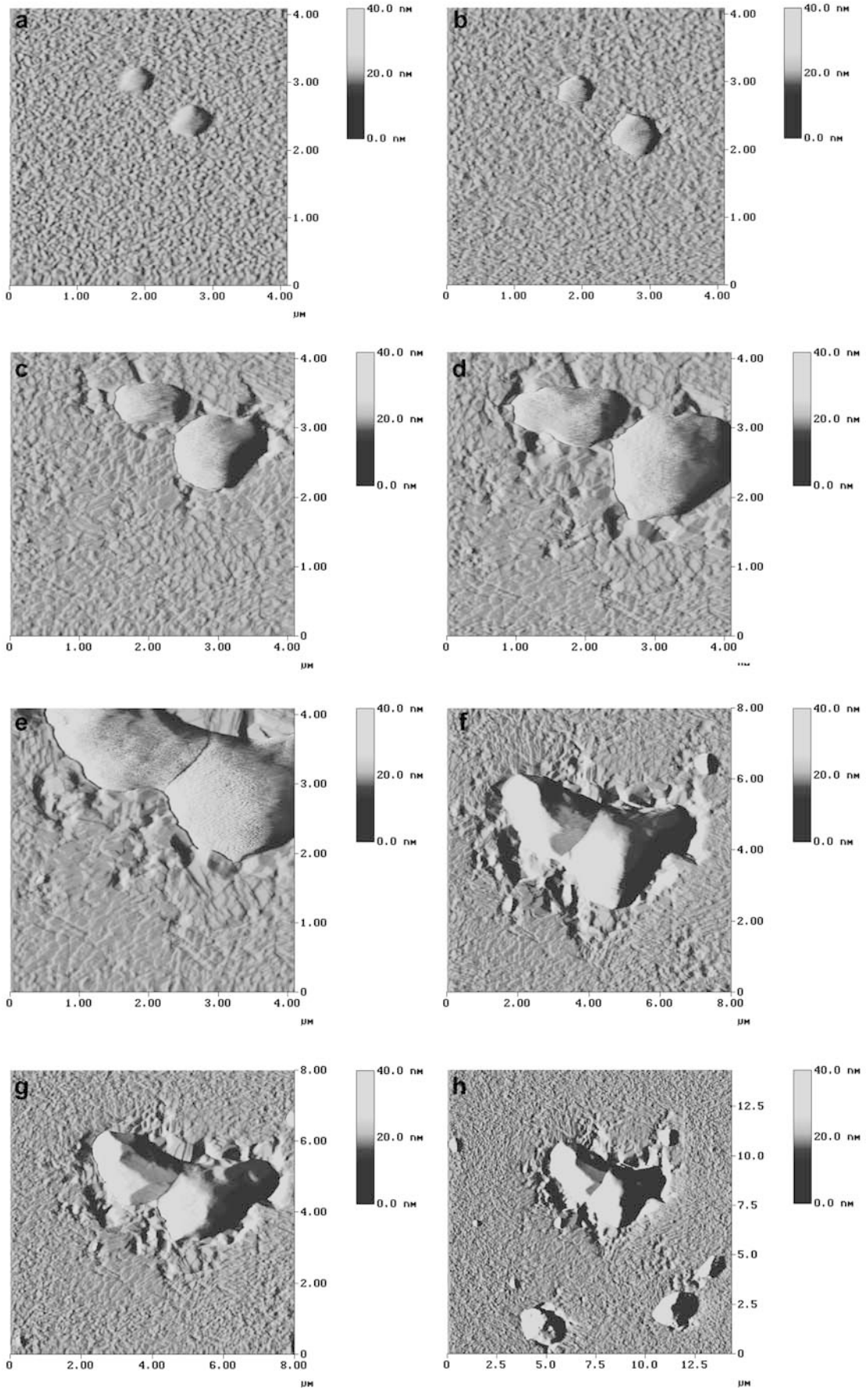
a
b
c
d
e
f
g
h
40.0 nm
20.0 nm
0.0 nm
μm

◀

Fig. 11a–h Atomic force micrographs of mercury(I) chloride crystal immobilized on a gold electrode in 0.1 potassium nitrate solution: **a** before, and **b** after a reduction at −700 mV for 5 s, **c** after a reduction for 10 s, **d** after a reduction for 15 s, **e** after a reduction for 20 s, **f** after a reduction for 25 s, **g** after a reduction for 30 s and **h** after a reduction for 35 s

screw dislocations because the transport rate of silver ions will be enhanced at such spots. There will be an additional flux of silver ions towards these dislocations that may be called $f_{Ag^+,screw}$. Not only may the transport rate of silver ions be enhanced, but the screw dislocation may also prompt the filamentous growth of silver for reasons of crystallographic nucleation. The probability of screw dislocations in the sub-micrometer size crystals would be rather small, whereas the probability for their occurrence in large crystals is much higher. Figure 14b schematically illustrates how a screw dislocation may be the locus for a whisker growth. The scenario depicted in Fig. 13b is in agreement with very early ideas developed by Jaenicke [13].

The reduction of immobilized silver halide crystals shows a remarkable difference to the scenario of reduction of immobilized lead oxide crystals, where it was observed that the reaction front proceeds through the entire crystal after having started at a three-phase junction line of just *one* edge of the immobilized crystals [4]. It can be speculated that the dissolution of oxide anions is much faster than that of halide anions because the O^{2-} will be protonated and irreversibly removed. Indeed, it was observed that the conversion of lead oxide crystals is much faster so that it was rather difficult to trap a partially reduced crystal. It is an intriguing

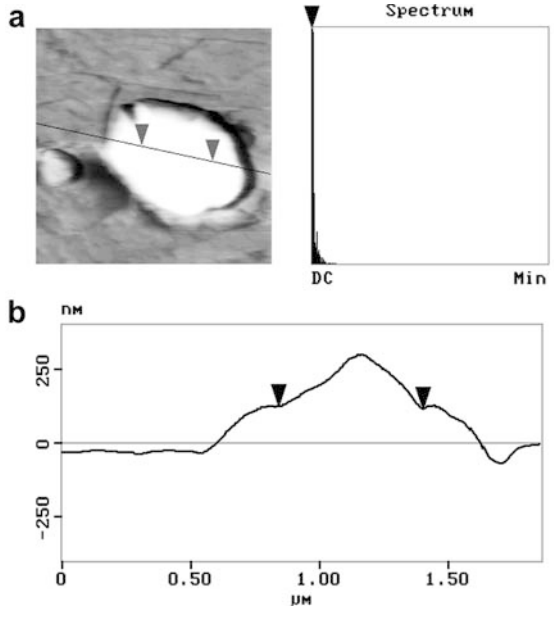

Fig. 12a, b Cut through a Hg_2Cl_2 crystal immobilized on a gold electrode after reduction at −700 mV for 5 s. The *arrows* indicate the reaction front where the liquid mercury borders the residual Hg_2Cl_2 crystal

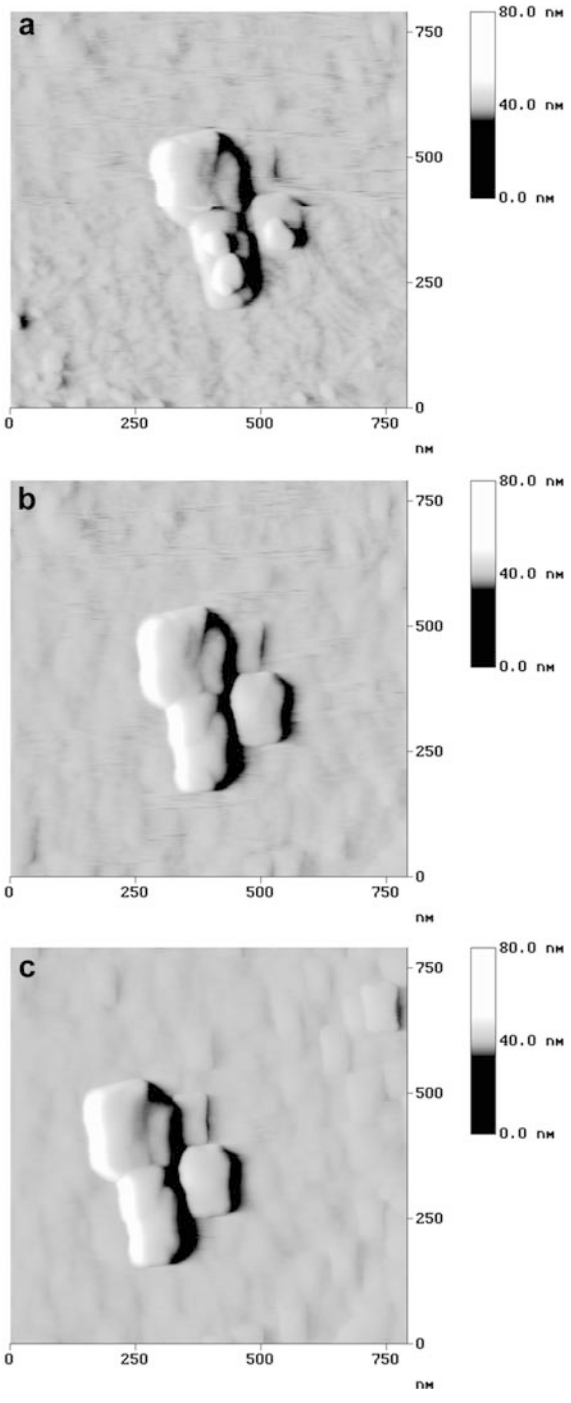

Fig. 13a–c Atomic force micrographs of mercury(I) chloride crystal immobilized on a platinum electrode in 0.1 potassium nitrate solution: **a** before, and **b** after a reduction at −700 mV for 5 s and **c** after a reduction for 10 s

question why the number of silver layers was, in all the experiments and with the different samples, rather constant. Of course, the data are averages and the thickness of the layers may somehow vary along the surface. However, it seems to be reasonable that the rate of transport of silver ions towards the silver layer (cf. Figure 14a) is responsible for the specific thickness of the silver layers.

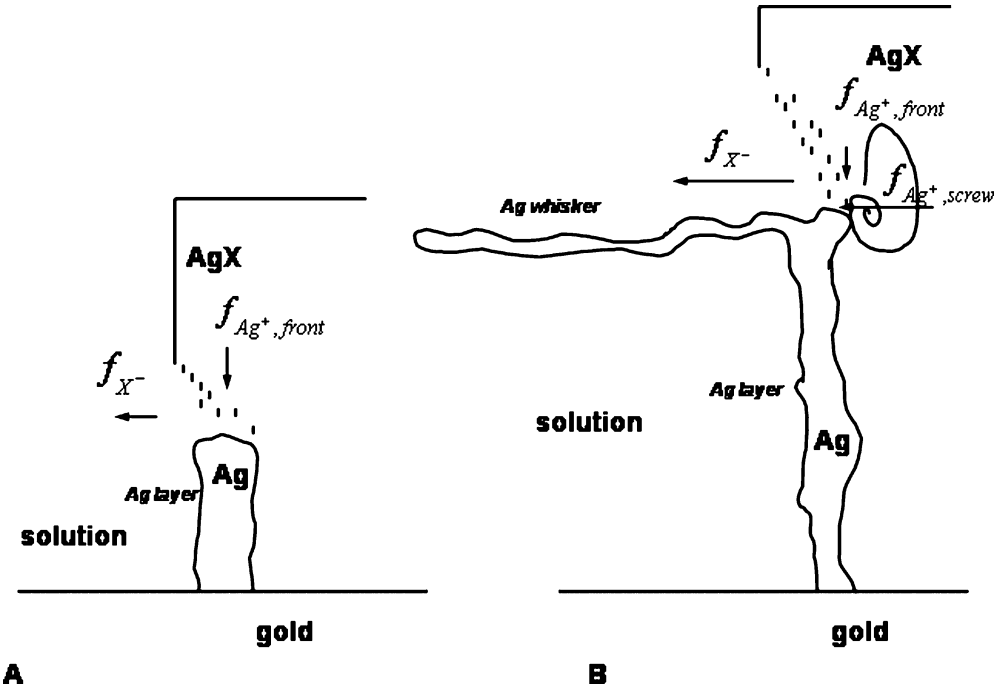

Fig. 14a, b Schematic drawing of the reduction of a silver halide crystal to silver. **a** Surface silvering of sub-micrometer size crystals (initial stage). **b** Whisker growth following to the initial formation of silver near to the three-phase junction after prolonged electrolysis of a *large* crystal. The *arrows* indicate the transport of silver ions to the silver | silver halide interface

It is very interesting that a chemical reducing agent, i.e., a usual chemical photo developer, completely reduced the entire immobilized silver halide crystal and produced a compact silver crystal instead of the well-known filamentous silver grains formed in photo emulsions. We conclude from this finding that the gold electrode acted here as the anode where the photo developer was oxidized. This role is played by silver grains of the latent image in a photo emulsion. We have no convincing arguments as to why the chemical reduction converted the entire crystals whereas the electrochemical reduction converted the surface only.

The mechanism of the reverse reaction, i.e. the oxidation of silver nanocrystals to silver halide crystals, follows a rather different pattern: the first in situ AFM experiments in which silver nanocrystals were oxidized to silver iodide and silver bromide, respectively, showed that the oxidation leads to a preliminary formation of an over saturated silver halide solution, from which only later do the silver halides precipitate on the electrode surface [14].

The results obtained for the reduction of mercury(I) halides immobilized on platinum electrodes are interesting because they show that the mercury indeed wets the surface of platinum. This result leaves the question why it is not possible to deposit from mercury solutions smooth mercury films on platinum.

It is worth comparing the reduction of silver and mercury halide crystals with the electrochemistry of immobilized droplets of organic solutions of electroactive compounds [15, 16, 17, 18, 19] and also with the electrochemical oxidation of white phosphorus [20]. In all these cases the three-phase junction was identified as the locus where the electrochemical reaction involving an electron and ion transfer starts. The present study of silver and mercury halides provides for the first time unambiguous proof that an electrochemical conversion of solid crystals indeed starts at a three-phase junction line.

Acknowledgements This project was supported by Deutsche Forschungsgemeinschaft. F. Sch. acknowledges supports by Fonds der Chemischen Industrie.

References

1. Bonnell DA (1993) Scanning tunneling microscopy and spectroscopy theory, techniques and applications. VCH, New York
2. Suárez MF, Marken F, Compton RG, Bond AM, Miao WJ, Raston CL (1999) J Phys Chem 103:5637
3. Suárez MF, Bond AM, Compton RG (1999) J Solid State Electrochem 4:24
4. Hasse U, Scholz F (2001) Electrochem Commun 3:429
5. Hasse U, Nießen J,Scholz F (2003) J Electroanal Chem 556:13
6. Frieser H, Haase G, Klein E (1968) Die Grundlagen der photographischen Prozesse mit Silberhalogeniden. Akademische Verlagsgesellschaft, Frankfurt am Main
7. James TH (1966) The theory of the photographic process. Macmillan, New York
8. Fyson JR, Twist PJ, Gould IR (2001) Electron transfer processes in silver halide photography. In: Balzani V (ed) Electron transfer in chemistry, vol 5., Wiley-VCH, Weinheim, pp 285–378
9. Lohmann J (1989) Angew Chem 28:1601
10. Mott NF, Gurney RW (1950) Electronic processes in ionic crystals, 2nd edn. Clarendon, Oxford, pp 237
11. Bard AJ, Parson R, Jordan J (1985) Standard potentials in aqueous solution. Dekker, New York
12. Jaworski A, Stojek Z, Scholz F (1993) J Electroanal Chem 354:1
13. Jaenicke W (1959) Z Elektrochem 63:722
14. Hasse U, Scholz F (2004) Electrochem Commun 6:409

15. Scholz F, Komorsky-Lovrić Š,Lovrić M (2000) Electrochem Commun 2:112
16. Gulaboski R, Mirčeski V, Scholz F (2002) Electrochem Commun 4:277
17. Donten M, Stojek Z, Scholz F (2002) Electrochem Commun 4:324
18. Scholz F, Gulaboski R, Caban K (2003) Electrochem Commun 5:929
19. Komorsky-Lovrić Š, Mirčeski V, Kabbe Ch, Scholz F (in press) J Electroanal Chem
20. Hermes M, Scholz F (2000) Electrochem Commun 2:845
21. See ref. [6], volume 1, p. 73